COMPARISON OF BRANCH EXTRACTION FOR DECIDUOUS SINGLE TREES IN LEAF-ON AND LEAF-OFF CONDITIONS – AN EIGENVECTOR BASED APPROACH FOR TERRESTRIAL LASER SCANNING POINT CLOUDS

Magnus Bremer[1,3], Andreas Jochem[2], and Martin Rutzinger[1,4]

1. University of Innsbruck, Department of Geography, Innsbruck, Austria; e-mail: magnus.bremer(at)student.uibk.ac.at, martin.rutzinger(at)uibk.ac.at
2. University of Heidelberg, Department of Geography, Heidelberg, Germany; e-mail: andreas.jochem(at)geog.uni-heidelberg.de
3. alpS, Centre for Climate Change Adaptation Technologies, Innsbruck, Austria; e-mail: bremer(at)alps-gmbh.com
4. Institute of Mountain Research: Man and Environment. Austrian Academy of Sciences, Innsbruck, Austria

ABSTRACT

Terrestrial Laser Scanning (TLS) is well suited to acquire high resolution point clouds, which can be used to derive single tree attributes for forestry applications. The processing of TLS point clouds requires the implementation of automated processing chains allowing operational data analysis in 3D. In order to obtain detailed information such as canopy structure, biomass and leaf area index and their respective changes over time the extracted branch structure of the tree is of particular interest. Based on TLS-point clouds a variety of procedures and workflows have been developed in order to extract branch parameters. Most approaches are limited by noisy data and inhomogeneous coverage within the canopy. This is mainly the case under leaf-on conditions were most branch segments are masked or under sampled.

We present an experimental framework for an automated processing chain for structuring and classifying TLS point cloud data into branches and foliage. The aim is the generation of improved input data for further sophisticated processing procedures such as skeletonization. By separating branches from leafs an improved input for branch hierarchy generation is expected. Branch extraction was done for an exemplary tree data set, which was acquired in summer (leaf-on) and winter (leaf-off) conditions respectively. First, segmentation of tree components inside of the TLS point cloud was performed. For each derived segment a corresponding structure tensor was computed, whereby eigenvectors and eigenvalues were derived. Applying a form-index describing the eigenvalue relationship for each segment, a classification into segment shapes has been done.

The quality of the extraction was tested under leaf-on and leaf-off conditions. Therefore, derived branch structures were analysed. It could be shown that major branch structures are derivable in both leaf-on and leaf-off conditions whereby small branches are more difficult to extract under leaf-on conditions. The algorithm shows good results in the reduction of noise from the data. However, large data gaps within the main branch system mainly due to occlusion in dense leaf-on canopy cannot be overcome by the current approach. Concluding, the presented approach cannot solve the problem of data gaps, but sufficiently unmasks branch structures of noisy data sets. It uses branch segments instead of point or voxel neighbourhoods for data representation and is a promising pre-processing approach for following procedures such as skeletonization and tree modelling of dense point clouds.

INTRODUCTION

The biological shape of vegetation structures and tree objects contains important information of particular relevance for ecophysiological research in forests or horticulture (1). In order to get detailed information on allometric tree species differences and tree healthiness, morphological parameters such as branch length and width, branching architectural patterns (ramification and branching angles) are of importance (1). Economical questions such as timber volume and biomass estimates are further potential applications (2). However, a manual collection of these features requires labour intense and time consuming fieldwork. Thus, the application of terrestrial laser scanning (TLS) is an advantage for a fast derivation of such parameters using computational efficient algorithms (3,4).

TLS is a method providing high resolution point measurements describing reflective surfaces of target objects in 3D space. The here used technique is based on a discrete recording time of flight measurement for emitted and received laser pulses. The laser pulses are emitted into varying directions controlled by two perpendicular mirror rotations. Combining orientation and range information for each pulse leads to the computation of an unorganized 3D point cloud.

The complexity of the derived geometrical point distribution increases with complexity of the target object and the point density. For tree objects the laser beam is able to penetrate through the canopy being reflected by various branch and leaf surfaces lying in its cross-section. In contrast to solid objects such as buildings or terrain surfaces a volumetric object is created, which appears as a complex multi surface layer situation in the point cloud.

While single points of a point cloud carry no structural object information themselves (3), object information has to be derived by data aggregation and classification algorithms based on point neighbourhood analysis. This is a challenging task for multi surface layer point clouds containing a lot of noise, varying point densities and occlusion effects (5,4).

In order to derive topological information from the complex hierarchical branching system of a tree, specialized algorithms such as tree-skeletonization procedures have been developed. Within these workflows the raw point cloud is simplified or pre-structured into subsets using voxel-gridding (4), octree subdivision (3,5,6) or segmentation (7) showing promising results for point cloud data. Thereby, the suitability of the extracted branch skeletons for the estimation of branch diameters and length could be shown (2). However, the presented workflows are still facing imperfect data representation. Although strategies including mathematical morphology (opening and closing) have been adapted in order to close data gaps (4), occlusion effects and masking noise - especially under leaf on conditions - are still limiting the extraction of salient and structured information from the data (4,5). Noise can be responsible for wrong connections in the constructed skeleton.

In order to overcome problems in noisy data and to extract salient information in 3D-point clouds or 2D-images, promising approaches from remote sensing, computational geometry and computer vision have been developed (7,8,9). The approaches are mainly based on the analysis of local-direction information. Especially for data hidden by a mask of noise and overlying structures the construction of a structure tensor can be a helpful tool for the derivation of dominating neighbourhood orientations (9). In the structure tensor specific neighbourhood characteristics can be encoded as described in the methods section. For the constructed tensor respective eigenvectors and eigenvalues can be computed using well established routines (10,11). As in 3-D space the structure tensor is constructed as a 3×3-covariance-matrix of a given neighbourhood (11), the eigenvectors and eigenvalues of this matrix can provide dimension and orientation information for this neighbourhood.

The structure tensor has also been used for orthogonal plane fitting algorithms, while the normal of the plane is the eigenvector to the smallest eigenvalue of the square matrix (2,11). However, the structure tensor is also capable to derive orientation and dimension information for volumetric objects: The three perpendicular eigenvectors derivable from the square matrix are describing orientated directions of the encoded data set allowing a shape classification by form-indices established for geological research questions (12,13). More isotropic and compact shape for leaf surfaces and elongated shapes for branch facets can be assumed. This offers an advantageous tool for branch extraction independent from intensity data. Additionally the longest eigenvector shows elongated branch orientation in 3D space (14).

In the presented work we are focusing on a new approach reducing influences of noise and occlusions for the extraction of structural tree information from TLS point clouds. The data-output is expected to provide more suitable data-output for further processing steps like skeleton computation and tree modelling. For the presented workflow an accuracy comparison under leaf-off and leaf-on conditions was carried out.

DATA

For the study an exemplary about 15 years old northern red oak (*quercus rubra*) was used for testing the developed workflow (Figure 1). The tree has a maximum height of 8.5 m and a stem diameter at breast height of 0.16 cm. Crown segments branching from the stem have maximal branch diameters of 7 cm.

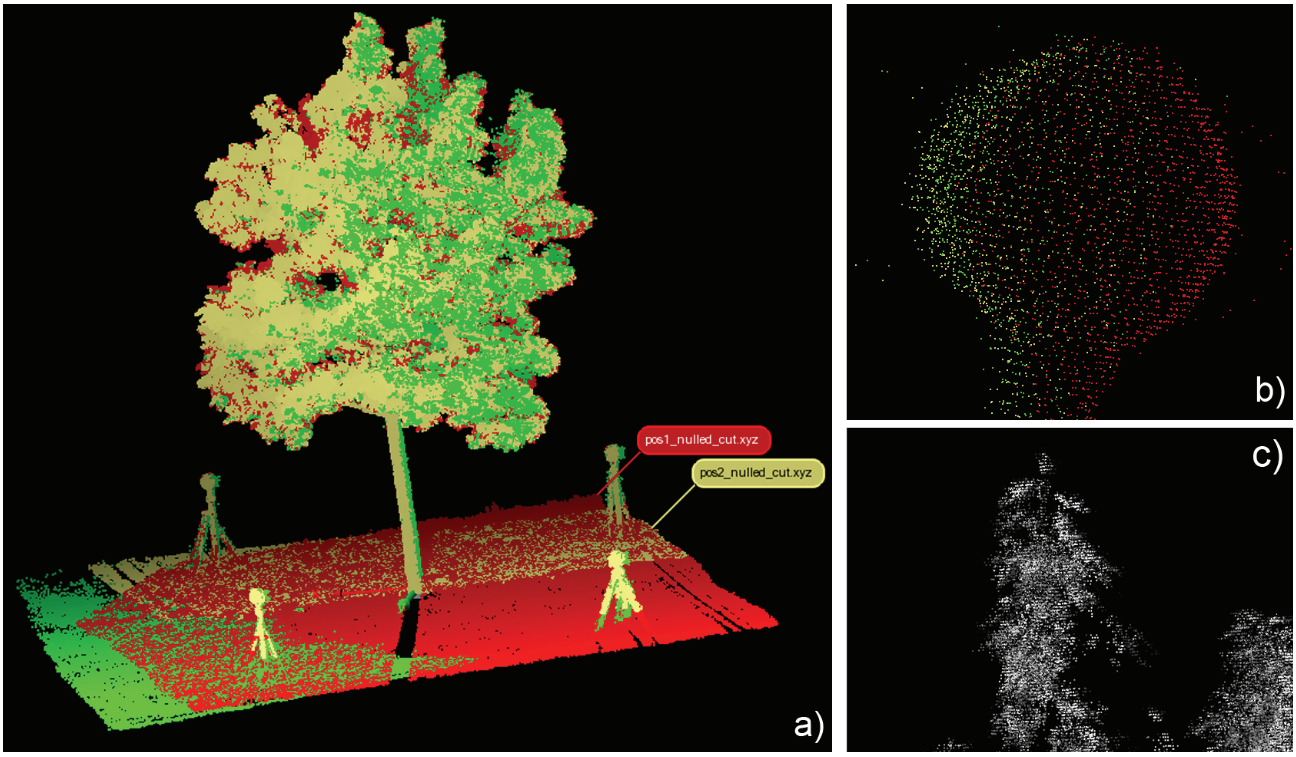

Figure 1: a) Registered point cloud for the leaf-on tree; b) registered point clouds for a sphere target with 20 cm diameter c) tree top within the leaf-on point cloud with signal intensities.

Point cloud data was acquired under leaf-on conditions at the 7th of October 2010 and under leaf-off conditions at the 10th of January 2011 with the discrete return recording Optech ILRIS-3D TLS. The employed instrument has a 40° × 40° field of view and a laser wavelength of 1535 nm. It can scan with a minimum step size of 20 µrad (0.001146°) and a beam divergence of 170 µrad (0.009740°). The raw range accuracy given by the manufacturer is defined as 7 mm at 100 m range.

To derive full 3D coverage of the tree under both leaf-on and leaf-off conditions, it was scanned from three different scan positions located in 120° steps on a radius of about 12 m around the tree stem.

The acquired scanner orientated point clouds of both phenological situations were prepared in the same way in order to enable geometrical comparisons. At first, the scanner oriented point clouds of both leaf-off and leaf-on situation were registered and merged into two separate project coordinate systems using sphere targets arranged around the tree. Therefore, the sphere objects were manually selected in each of the scanner oriented point clouds using the software Innovmetric Polyworks. The selected point sets served as input for the least square fitting of sphere primitives where the sphere centres were used as tie points for the registration process. The quality of the fit for the selected data points results in RMS errors between 4 and 7 mm and a standard deviation between 5 and 7 mm. The same order of magnitude for the RMS error and the standard deviation of the spherical fit is found for the merged project point cloud indicating a sufficient high accuracy for this kind of application (Table 1).

Table 1: Quality parameters for the registration of scan position point clouds

	sphere fitting parameters		plane fitting parameters
	leaf-off	leaf-on	matched point clouds
RMS-Error	0.004 - 0.006 m	0.005 - 0.006 m	0.003 - 0.006 m
standard deviation	0.004 - 0.006 m	0.004 - 0.006 m	0.004 - 0.006 m

Additionally, a house wall beside the observed tree was used to fit in planes into the point cloud in order to quantify the overall positional accuracy of the data points deviating from the plane. There, the RMS error and the standard deviation resulted 3 to 4 mm.

Finally, the leaf-off and leaf-on project point clouds were matched (IMAlign module of Innovmetric Polyworks) using the same house wall. Quantifying differences between the fitted plane at the house wall and the matched data points showed an RMS error and a standard deviation of 4 to 6 cm. The matching allowed a direct visual and computational comparison of both phenological situations in the 3D space.

In order to derive a reliable reference data set representing the main branches of the observed tree, the leaf-off point cloud was reduced by manual selection. Thereby, all branches showing smaller branch diameters than 1 cm in reality and up to 4 cm in the point cloud were treated as noise and deleted.

METHODS

The applied workflow includes a pre-structuring of point subsets, computation of a structure tensors for each subset, shape characterisation and shape filtering (Figure 2).

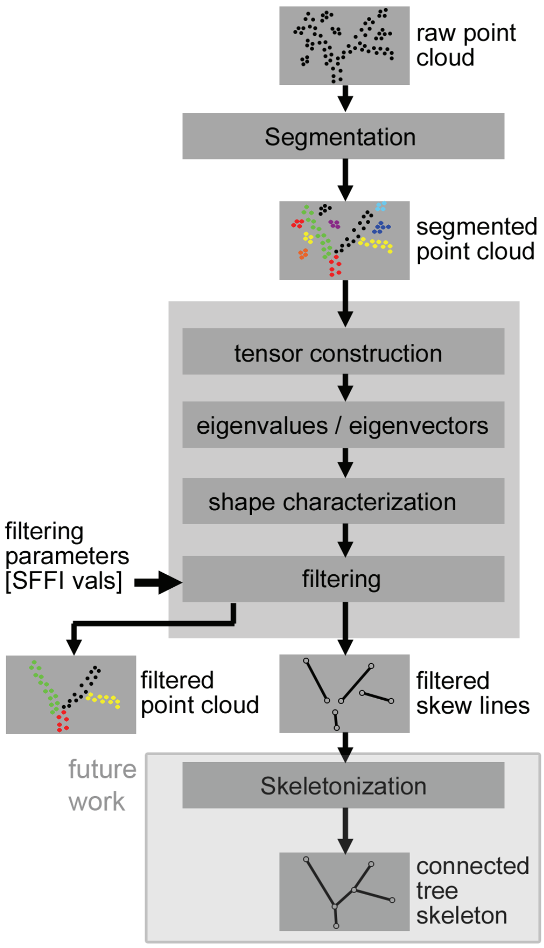

Figure 2: Workflow for branch extraction.

Pre-Structuring / Segmentation

For extracting main branches from the data, the raw input point cloud is pre-structured by a surface growing algorithm. Therefore, we assumed the tree object to consist of multiple planar branch and leaf surfaces enlighted by the laser beam. Doing so, branches are represented by elongated prisms showing differently oriented facets. For TLS data sufficient point density is available for branch surface description (2) confirmable in the visual inspection of the data points. Thus, we pre-structured the point data into point sub sets aggregating points belonging to one planar surface facet. For this process the point cloud is segmented into planar sub sets using a surface growing algorithm (15). Thereby, points showing less difference than 2 cm towards a respective plane were added to a growing point cloud segment and labelled with a segment number. All points not fitting into a planar segment were ignored for further processing steps.

Structure tensor and shape filtering

In the second step we used an algorithm reading the data points per subset, computing the structure tensor and applying a shape characterization. In the end of the procedure a filter criterion is applied in order extract elongated segments i.e. branches from more isotropic features such as leafs.

We encoded the geometrical information of *k* points in each subset into a structure tensor storing orientation and position information and providing a description of each point neighbourhood (10). For the construction of the tensor the point coordinates reduced to the centroid of the *k* points were written as a matrix (*A*). Multiplying A^T with *A* the 3x3 square matrix was constructed:

$$A = \begin{bmatrix} x_1-\bar{x} & y_1-\bar{y} & z_1-\bar{z} \\ . & . & . \\ . & . & . \\ . & . & . \\ x_k & y_k & z_k \end{bmatrix}$$

$$A^T A = \begin{bmatrix} \sum_{i=1}^{m}(x_i-\bar{x})^2 & \sum_{i=1}^{m}(x_i-\bar{x})(y_i-\bar{y}) & \sum_{i=1}^{m}(x_i-\bar{x})(z_i-\bar{z}) \\ \sum_{i=1}^{m}(x_i-\bar{x})(y_i-\bar{y}) & \sum_{i=1}^{m}(y_i-\bar{y})^2 & \sum_{i=1}^{m}(y_i-\bar{y})(z_i-\bar{z}) \\ \sum_{i=1}^{m}(x_i-\bar{x})(z_i-\bar{z}) & \sum_{i=1}^{m}(y_i-\bar{y})(z_i-\bar{z}) & \sum_{i=1}^{m}(z_i-\bar{z})^2 \end{bmatrix}$$

Deriving eigenvectors and eigenvalues for each structure tensor, we applied the Sneed & Folk Form Indices (SFFI) (13) in order to characterize segment shapes (Figure 3). Thereby, each point segment was labelled with its shape characterization (SFFIx / SFFIy). SFFI makes it possible to apply variable threshold parameters in order to extract elongated branch segments. For an optimized branch extraction the best performing threshold parameters were tested in comparison to the manually selected reference model.

The accepted point segments were stored object wise as a cloud of single skew lines in 3D space. As the longest eigenvector stores the orientation of the elongated segments in 3D (14) skew lines were computed for the elongated segments using intersections of the longest eigenvector with the bounding box of the segment as start- and endpoints. The start and endpoints of these skew lines could serve as vertices to be connected in a specially adapted skeletonization algorithm. Simplifying the input point cloud to a filtered cloud of skew lines reduced the amount of 1462880 data points to just 830 lines (for the leaf-off tree). Thereby, a skew line as a branch object representation can describe length and orientation of a branch segment in 3D space and serves as a practical alternative towards other data representations such as voxel structures or octree subdivisions.

Additionally, each data point belonging to an accepted point segment was labelled with its direction information and stored in a filtered point cloud. This will allow a skeleton computation and data analysis on basis of the line set in future work.

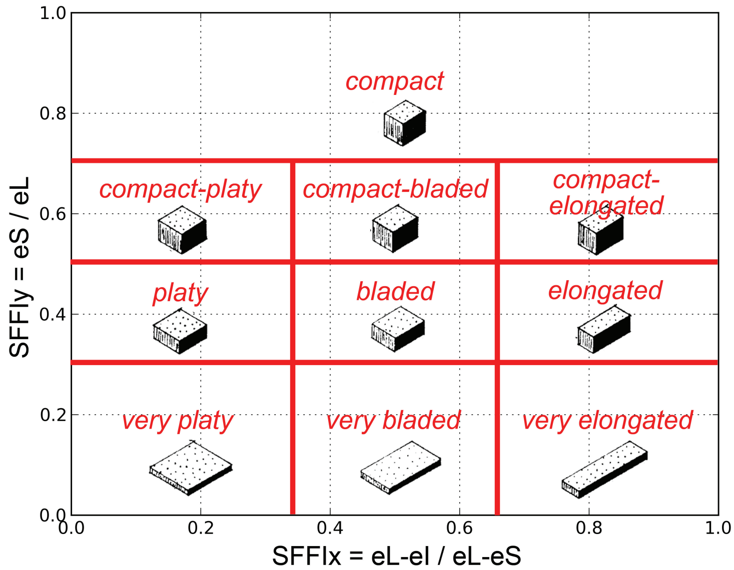

Figure 3: Sneed and Folk Form Diagram showing different shape classes with varying SFFI-values between 0 and 1 (eL = longest eigenvector, eI = intermediate eigenvector, eS = shortest eigenvector.)

RESULTS

The results of the segmentation algorithm show a fragmentation of the raw point clouds into small planar point subset of varying dimension and orientation (Figures 4-6). Comparing the results of the leaf-on, leaf-off and reference tree different shape patterns of foliage and branch segments can be observed in both visual inspection of the point cloud and the form classification results (Figure 4). The leaf on tree shows a variety of isotropic segments in its canopy while most segments of the leaf-off and reference tree are elongated branch facets. For the leaf-on tree the main branch system is occluded by dense foliage. The leaf-off tree contains several small branches of increased thickness compared to reality (1-2 cm diameters are increased to 3-6 cm in the point cloud). The main branch system is occluded by these overlying structures in both leaf-on and leaf-off data making a reliable branch extraction more difficult.

These characteristics can also be visualized by plotting SFFIx and SFFIy values for the unfiltered leaf-on, unfiltered leaf-off and reference tree in form diagrams (12). Most segments of the three tree representations have a platy shape with SFFIy values smaller than 0.4. This is due to the segmentation procedure, creating point segments of planar shape. Comparing the reference and the leaf-off tree shows an increased appearance of elongated segments with SFFIx values greater than 0.7 and SFFIy values smaller than 0.1. In particular the reference tree objects are plotting completely in the lower right corner of the diagram indicating very elongated objects. In contrast to this the leaf-on tree contains several isotropic surface segments representing leafs (SFFIx > 0.25; SFFIy < 0.2) that have to be filtered out.

The presented shape filtering algorithm was evaluated for different input parameters including SFFIx, SFFIy, and the length of an accepted segment. Therefore the reference tree point cloud was compared to the filtered point cloud computing true positive, false positive and false negative values in order to derive completeness and correctness of the filter result (16).

For the assessment of the best parameters two criterions were used: i) as the reference tree was selected from the leaf-off tree, both representations show direct point to point correspondences allowing a direct relation of reference point cloud and filtered point cloud. Thus, each point showing a counterpart in the other data set is considered as true-positive (TP), (ii) for the comparison of the reference tree with the leaf-on tree no direct point to point correspondences are given. Therefore we used a second evaluation criterion considering all points with a neighbour in the other data set in a 2.5 cm radius as TP (true positive).

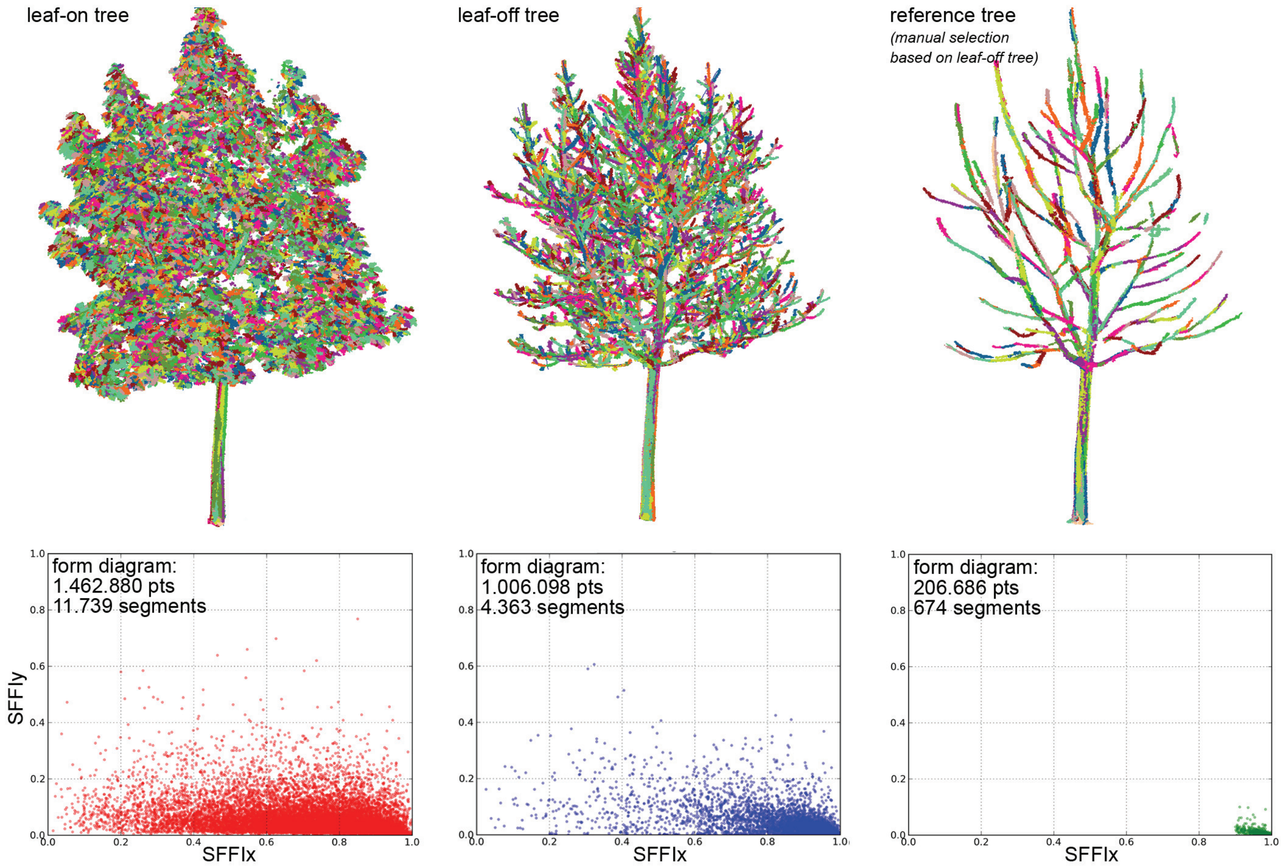

Figure 4: Comparison of leaf-on, leaf-off, and reference tree segmentation in 3D view and the form diagram; the form diagram shows the shape distribution of the created segments. SFFIy (1 = volumetric; 0 = not volumetric (plane/line)) and SFFIx (1=line shape / 0=plane shape) indicate the shape.

Best filtering parameters were indicated by computing completeness, correctness and quality from TP, FN (false negatives) and FP (false positives):

1. Completeness = TP / TP + FN
2. Correctness = TP / TP + FP
3. Quality = TP / TP + FN + FP

For the leaf-off tree the best filtering parameters were a SFFIx of 0.7, a SFFIy of 0.1 and a length threshold of 0.25 cm. Thereby, for the first criterion an amount of 155637 correctly represented points in the filter product could be stated. The completeness and correctness amounted for 0.76 and 0.46. For the second criterion correctly represented points amounted to 205222 points, leading to a completeness of 0.99 and a correctness of 0.67 (Table 2).

The visual inspection shows good results: The noisy structures are clearly decreased; The unmasked branch system shows a sufficient coverage with data points and hardly any data gaps (Figure 5).

For the leaf-on tree the best parameters were a SFFIx of 0.9, a SFFIy of 0.1 and a length threshold of 0.2 cm. The completeness (0.70) and correctness (0.67) accuracies show, that the filtered point cloud less sufficiently represents the main branch system (Table 2). While most overlying structures and noise could be reduced, this is mainly due to under sampling in the leaf-on point cloud causing large data gaps within the canopy. The under sampling is caused by dense foliage minimizing the chance for the laser beam to hit a branch object. Thus, the incomplete coverage is complicating branch extraction (Figure 6).

Table 2: accuracy assessment for the filtering approach using optimal parameters: (leaf-off) SFFIx = 0.7, SFFIy = 0.1; (leaf-on) SFFIx = 0.9, SFFIy = 0.1.

	leaf-off (1006098 pts)		leaf-on (1462880 pts)
	point in radius correspondence (r = 2.5 cm)	point to point correspondence	point in radius correspondence (r = 2.5 cm)
TP count (ref: 206686 pts)	205222	155637	146434
completeness	0.99	0.76	0.70
correctness	0.67	0.46	0.67
quality	0.66	0.39	0.58

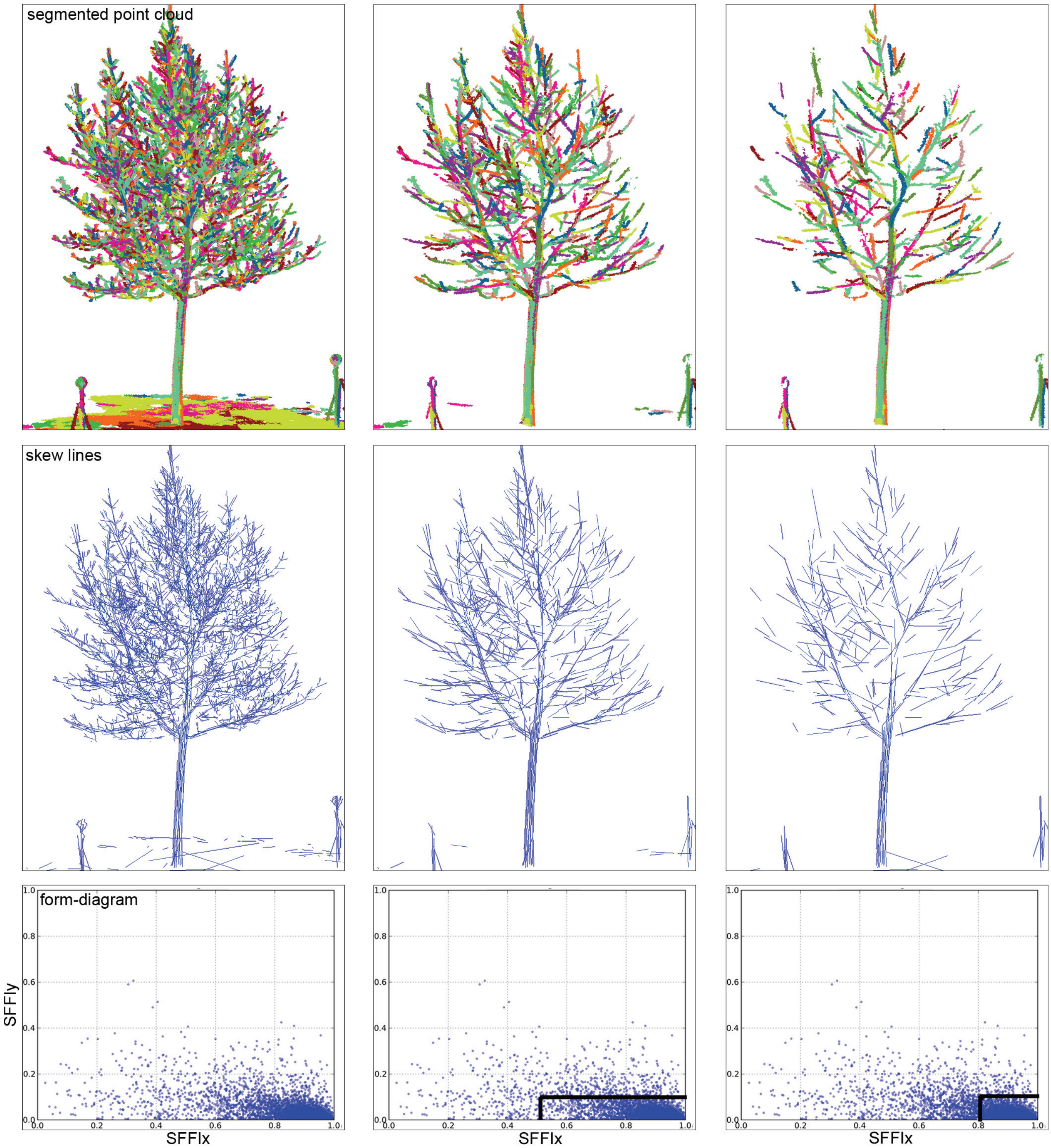

Figure 5: Comparison of different filter results for the leaf-off data set: a) No filtering [SFFIx = 0, SFFIy = 1]); b) filtering with SFFIx = 0.7 and SFFIy = 0.1; c) filtering with SFFIx = 0.9 and SFFIy = 0.1.

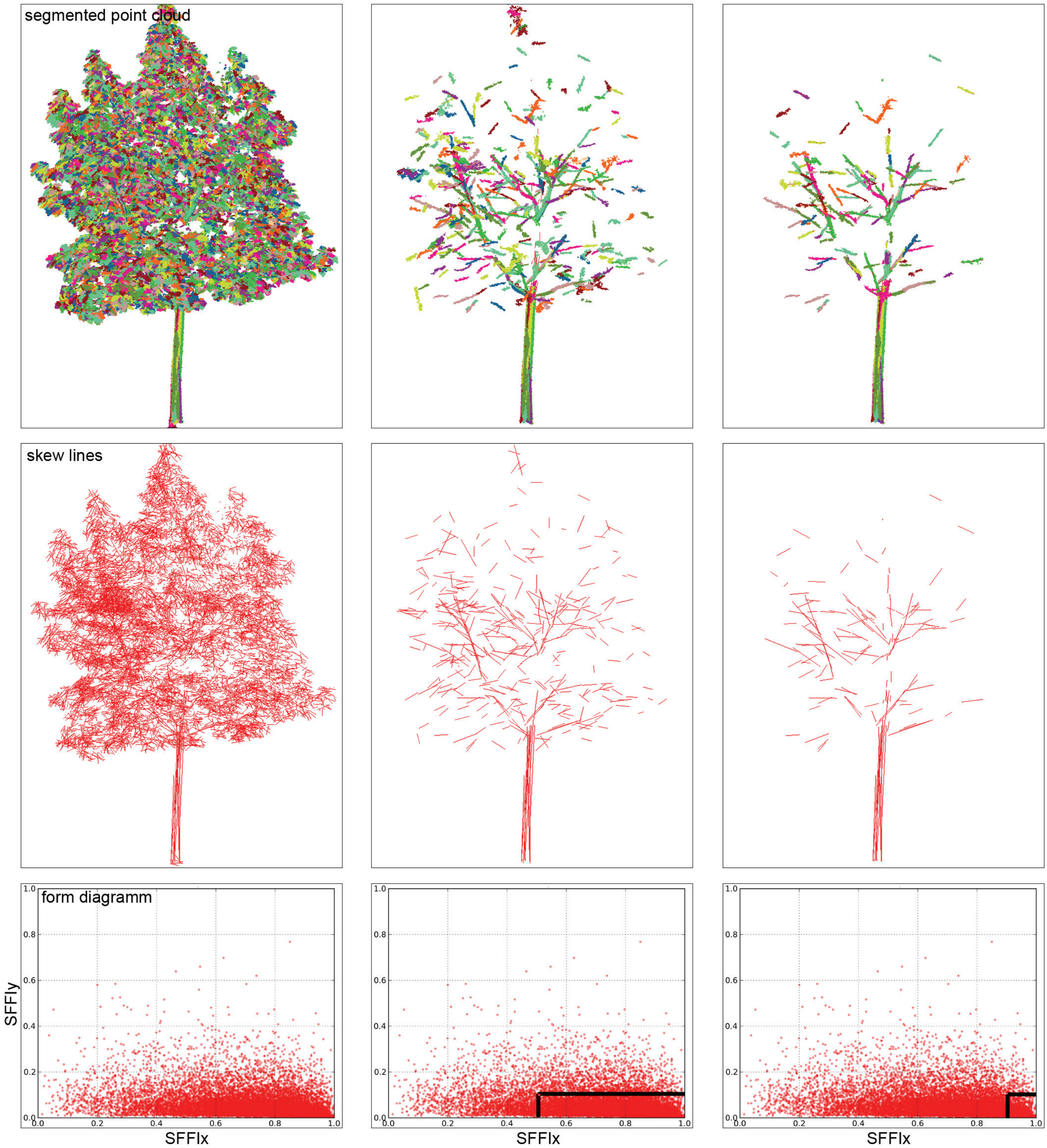

Figure 6: Comparison of different filter results for the leaf-on data set: a) No filtering [SFFIx = 0, SFFIy = 1]); b) filtering with SFFIx = 0.7 and SFFIy = 0.1; c) filtering with SFFIx = 0.9 and SFFIy = 0.1.

CONCLUSIONS

The main difficulties for detailed branch extraction and hierarchy derivation from trees based on TLS-data are (i) inhomogeneous point densities or data gaps and (ii) noise structures within the data (2,5). The aim of this study was to minimize these influences using a specific filter approach. Generating segment-based data representation allowed to simplify the raw point-cloud data and improved data handling. In future, this improved and simplified data can be useful for fast skeletisation and tree-modelling procedures.

The performance of the presented simplification and improvement method varies under leaf-off and leaf-on conditions. The leaf-on tree shows a variety of noise structures but is mainly influenced by data gaps within foliage. While these data gaps are determined by the characteristics of the survey constellation including scanner performance, scan angles and scan positions, these difficulties could not be decisively minimized by the presented processing approach. The example tree is rather young and therefore has small branches with a diameter of less than 5 cm, showing a low possibility for branch detection. Since the diameter is in the order of the TLS scanning precision it is difficult to detect branches with the applied scanning constellation. Using a scanner instrument capable to measure only one return per emitted pulse was a further limiting factor for sufficient coverage and filtering.

In contrast to the problem of occlusions we could achieve good results for noise reduction. This could be shown for both the leaf-off tree and the leaf-on tree. However, the best results were obtained for the leaf-off tree, were the main branches show sufficient coverage.

Concluding, the presented approach cannot overcome entirely the occurrence of data gaps, but sufficiently unmasks branch structures in noisy data sets providing improved input data for other processing steps (e. g. skeletonization). Future work will focus on the execution of the workflow for building up a branch skeleton, which is the input for tree modelling. Additionally, the combination of the presented filtering approach with signal-intensity-based filtering might improve noise and leaf elimination.

ACKNOWLEDGEMENTS

This research was partly funded by the project K3B (Research Centre Mountain Agriculture Research Unit, University of Innsbruck). It is embedded into the doctoral scholarship of the University of Innsbruck.

REFERENCES

1 Fleck S, D van der Zande, M Schmidt & P Coppin, 2004. Reconstructions of tree structures from laser scans and their use to predict physiological properties and processes in canopies. International Archives of Photogrammetry, Remote Sensing and Spatial Information Sciences, XXXVI-8/W2: 119-123

2 Pfeifer N, B Gorte & D Winterhalder, 2004. Automatic reconstruction of single trees from terrestrial laser scanner data. International Archives of Photogrammetry, Remote Sensing and Spatial Information Sciences, XXXV, part B5: 114-119

3 Bucksch A & R Lindenbergh, 2008. Campino – a skeletonization method for point cloud processing. ISPRS Journal of Photogrammetry and Remote Sensing, 63(1): 115-127

4 Gorte B & N Pfeifer, 2004. Structuring laser-scanned trees using 3D mathematical morphology. International Archives of Photogrammetry, Remote Sensing and Spatial Information Sciences, XXXV, part B5: 929-933

5 Bucksch A, R Lindenbergh & M Menenti, 2010. SkelTre - Robust skeleton extraction from imperfect point clouds. The Visual Computer, 26: 1283-1300

6 Bucksch A, R Lindenbergh & M Menenti, 2009. SkelTre – Fast skeletonisation of imperfect point clouds of botanic trees. In: Proceedings 3D Object Retrieval Workshop 2009 (3DOR), 13-20

7 Dai M, H Li & X Zhang, 2010. Tree modeling through range image segmentation and 3D shape analysis. Advances in Neural Network Analysis and Applications, 67: 413-422

8 Dai M, X Zhang, Y Zhang & M Jaeger, 2010. Segmentation of point cloud scanned from trees. In: Computer Vision – ACCV 2009, edited by H Zha, R Taniguchi & S Maybank (Springer, Berlin) 390 pp., 1-12

9 Haußecker H & B Jähne, 1996. A tensor approach for local structure analysis in multidimensional images. In: Proceedings 3D Image Analysis and Synthesis '96, edited by B Girod, H Niemann & H P Seidel (Erlangen, Germany) 171-178

10 Golub G H & C F van Loan, 1996. Matrix Computations, (The John Hopkins University Press, Baltimore, MD) 694 pp.

11 Shakarji, C M, 1998. Least-squares fitting algorithms of the NIST algorithm testing system. Journal of Research of NIST, 103: 633-641

12 Sneed E D & R L Folk, 1958. Pebbles in the lower Colorado River, Texas, a study of particle morphogenesis. Journal of Geology, 66: 114-150

13 Zingg T, 1935. Beitrag zur Schotteranalyse. Schweizerische Mineralogische und Petrographische Mitteilungen, 15: 39-140

14 Bienert A, R Queck, Schmidt A, C Bernhofer & H G Maas, 2010. Voxel space analysis of terrestrial laser scans in forests for wind field modelling. ISPRS Archives, XXXVIII, part 5: 929-933

15 Vosselman G & R Klein, 2010.Airborne and Terrestrial Laser Scanning, edited by G Vosselman, H-G Maas (Whitles Publishing, Dunbeath), 318 pp., chapter 2, 43-79

16 Leitloff J, S Hinz & U Stilla, 2005. Vehicle queue detection in satellite images of urban areas. ISPRS Archives, XXXVI-8/W27, 5 pp.